Vol. 6, No. 2, pp. 197-219, (June 2025)
DOI: 10.21608/aujes.2025.380878.1345
Aswan University Journal of Environmental Studies (AUJES)
Online ISSN: 2735-4237, Print ISSN: 2735-4229
Journal homepage: https://aujes.journals.ekb.eg/ E-mail: AUJES@aswu.edu.eg
Original research

Removal of Lead and Iron from polluted water by adsorption on peanut shell adsorbent

Aya Mohammed Naguib[1], Mohamed Nageeb Rashed[2,*], Kassem Ahmed Said[1] , Noura Sharkawi Abazeid[3]

1.Natural Resources Department, Institute of African and Nile States Researches and Studies, Aswan University
2.Chemistry Department, Faculty of Science ,Aswan University
3. Botany department , Faculty of science , Aswan university

Received:19 /3 /2025 Accepted: 1 / 4 /2025

Abstract:

Due to their non-biodegradable and tendency to bioaccumulate, heavy metals pose a significant danger to aquatic ecosystems. The purpose of this study is preparation of peanutshell biosorbent and investigation of the efficacy of this adsorbent in the heavy metals (Pb and Fe) removal from polluted water. The peanut shell adsorbent was prepared by different methods including physical activation by calcination at 300°C, 500°C and 800°C, chemical activation using 1M HCl, H_3PO_4 and NaOH , and physical activation followed by chemical activation. The adsorption test results for Pb and Fe showed that the adsorbent prepared by calcination at 800 °C followed by chemical treatment with 1M NaOH showed higher Pb and Fe removal than with the other activators. The selected adsorbent was analyzed using XRD, SEM, EDX, BET,and FTIR. High removal efficiency of Pb ions adsorption were 50 mg/l metal concentration, pH 5, solution temperature 323 K, contact time 30 min, and 0.5g adsorbent dose, while that for Fe removal it was observed at 50 mg/l metal concentration, pH 5, temperature 303 K, contact time 90 min, and 0.1 g of adsorbent. Adsorption of Pb and Fe ions were found to be well fit to Langmuir and Freundlich isotherms, and the pseudo second order kinetic model for both removal heavy metals. Pb and Fe adsorption on the prepared adsorbent was endothermic and spontaneous process. The resulted absorbent was successfully applied for the removal of Pb and Fe ions from water of Lake Nasser and Lake Nubia.

Keywords: heavy metals ; adsorbent ; peanutshells ; pollution

1- Introduction

Water is a fundamental resource for sustaining life on Earth. Safe drinking and usable water should be colorless, odorless, and tasteless, while containing essential minerals such as Ca, Mg, and Na. It should not contain harmful microorganisms, heavy metals, nitrites, nitrates, or organic matter (Kılıç, 2020). However, in recent decades, water quality has deteriorated due to factors such as rapid population growth, industrialization, irresponsible exploitation of natural resources , and urbanization (Vardhan et al., 2019; Carolin et al., 2017).

Corresponding author*: E-mail address: mnrashed@aswu.edu.eg

Water pollution endangers the lives of all aquatic organisms and damages biodiversity in oceans, seas, lakes, and other aquatic ecosystems . Pollution affects more than just water; it also affects soil, which is then transferred to plants, fruits, and vegetables through irrigation. Animals that consume this water are also impacted. Utilizing contaminated water causes illnesses in a variety of species, lowers agricultural output, raises mortality, and raises the expense of treating drinking and utility water (Kılıç, 2020). The contaminants associated with water pollution fall into four categories: organic and inorganic contaminants, radiological contaminants, and biological contaminants (Sharma and Bhattacharya, 2017):

Heavy metals and metalloids are inorganic contaminants such as Cu, Cd, Zn, Pb, Hg, As, Ag, Cr, Fe, and Pt. These harmful metals are frequently discharged into water from a variety of natural and human-made sources (Ledezma et al., 2021). Lead is a toxic metal recognized as harmful to human health when inhaled or ingested. The Environmental Protection Agency has set the maximum contamination level objective for lead in drinking water at zero, even at low exposure levels.. Although iron is not considered hazardous to health and is essential for transporting oxygen in the blood, it is regarded as a secondary or "aesthetic" contaminant under Department of Natural Resources guidelines, and the recommended limit for Fe in water is 0.3 mg/L.

As heavy metals pose significant threats to all forms of life and the environment, it is crucial to remove these toxic metals from wastewater before discharge to avoid further harm (Hussain et al., 2021). Different techniques applied for removal of heavy metals from contaminated water as ion exchange , reverse osmosis , coagulation , chemical precipitation , membrane filtration, flocculation, electrochemical, electrolysis , biological methods ,phytoremediation and adsorption. Traditional methods for removing heavy metals from wastewater often face drawbacks such as low efficiency, high energy consumption, generation of toxic residues, and cost ineffectiveness (Barakat , 2011). Adsorption is an alternative technique that has been investigated to overcome these limitations. It involves the transfer of adsorbate molecules from a solution to the surface of an adsorbent (Hussain, 2021). Adsorption is favored for heavy metal removal due to its ease of use, high removal efficiency across various pH levels, and low cost (Madhubashani et al., 2021). Adsorbents can often be regenerated and reused (Ojedokun and Bello, 2016). Adsorption is considered environmentally friendly as it does not produce toxic pollutants (Demirbas, 2008).To enhance sustainability in wastewater treatment, it is essential to develop and use adsorbents that are readily available, inexpensive, and renewable (Bello et al., 2013). Key criteria for selecting adsorbents include cost-effectiveness, high surface area, porosity, and the presence of functional groups with favorable polarity (Ewecharoen et al., 2009; Vunain et al., 2016). Recent advancements have focused on developing various low-cost adsorbents from agricultural waste. Peanut shells, which are the residual product obtained after the removal of groundnut seeds from their pods, represent a substantial agricultural by-product that decomposes slowly under natural conditions (Zheng et al., 2013). These shells are often discarded as agro-waste following the extraction of the usable pods. Peanut shells, known for their macroporous structure and resistance to temperature fluctuations, pH changes, mechanical stress, and prolonged immersion in water, have proven effective in treating wastewater to remove As, Cd, Cr,Cu, Pb, Ni and Zn (Husaini et al 2011).

The aim of this study is to prepare low cost adsorbent from Peanut shells. Activation methods were used include 1- physical activation by calcination at 300 ^{o}C , 500 ^{o}C and 800 ^{o}C, 2- chemical activation by 1M HCl, H_3PO_4 and NaOH , and 3- physical activation followed by

chemical activation. . Following synthesis, the adsorbents' physical and surface characteristics were evaluated. The effects of adsorbent dose, temperature, time, pH, and metal concentration on the removal of Pb and Fe using the prepared adsorbents were investigated.

2- Materials and method

2.1. Chemicals and Reagents

High analytical grade chemicals and reagents HCl, H_3PO_4 , NaOH , $Pb(NO_3)_2$ and $Fe(NO_3)_2$,Merk and BDH) , were used.

2.2. Preparation of metal ions standard solution

1000 mg/l standard solutions Pb^{2+} and Fe^{2+} ions were prepared using $Pb(NO_3)_2$ and $Fe(NO_3)_2$. Working standard solution were prepared by diluting the stock ones.

2.3. Peanut shell sample collection:

Peanut shells were obtained from the local market in Aswan, Egypt. The located material was thoroughly washed with tap water followed by distilled water to eliminate any dirt particles. After washing, it was air-dried at room temperature and subsequently oven-dried at 105 °C for 24 hr. Once dried, the shells were ground into a fine powder, sieved through a 0.8 mm mesh, and stored in an airtight container for use in experiments.

2.4. Preparation of peanut shell adsorbent:

Peanut shell adsorbents were prepared using three methods:, physical activation by carbonizationو chemical activation, and physical followed chemical activation. For Method 1, physical activation by carbonization appropriate amounts of peanut shell powder was carbonized at 300 °C, 500 °C, and 800 °C, respectively, for 1 hour. The products obtained at different temperatures were labeled as PSt . for method 2 chemical activation of peanut shell, 2 grams of the peanut shell powder was activated with 50 mL 1 M activator (HCl, H_3PO_4 and NaOH) . The mixture was stirred for 24 hours on a magnetic stirrer at 150 rpm. After stirring, the solution was filtered. The filter was then washed repeatedly with distilled water until the filtrate was neutral. Finally, the treated peanut shell was dried in an oven at 105°C until a constant weight was achieved, approximately 24 hours. The products obtained were labelled as PS_{HCl} , PS_{H3PO4} , and PS_{NaOH} . For method 3 Physical activation followed by chemical activation , the collected biochar (PSt) were chemically activated using 1 M HCl, H_3PO_4 and NaOH. Specifically, 2 gm of PSt adsorbent was suspended in 50 mL of each 1 M HCl, H_3PO_4 and NaOH. The suspensions were stirred for 24 hours at room .temperature. After treatment, the biochar was filtered and washed several times with deionized water until the pH of the wash water reached neutrality. The washed biochar was then dried at 105°C overnight. The chemically modified biochar samples were labeled as $PS_{300,HCl}$, $PS_{300,H3PO4}$, $PS_{300,NaOH}$, $PS_{500,HCl}$, $PS_{500,H3PO4}$, $PS_{500,NaOH}$, $PS_{800,HCl}$, $PS_{800,H3PO4}$ and $PS_{800,NaOH}$, respectively.

2.5. Morphological charachterization of adsorbents:

The activated peanut shell was characterized by SEM/EDX (via ZEISS Sigma 500VP FE-SEM high-resolution scanning electron microscope) , BET (Tristar2 3020, Micromeritics, USA) , XRD (XRD, Bruker co D8, Germany) instrument) and FTIR (Cary 630 FTIR spectrometer, produced by Agilent Technologies.) .

The metal ion concentrations were determined using Atomic absorption spectrometery, AAS (Thermo Scientific ICE 3000 series)

2.6. Adsorption experiments

2.6.1. A comparative study for the adsorption of Pb^{2+} and Fe^{2+} by the prepared peanut shell adsorbents

Batch experiments of Pb^{2+} and Fe^{2+} adsorption onto the prepared peanut shell adsorbents were performed using 0.25 g adsorbent stirred with 25 ml of 50 ppm metal ion solution at room temperature, pH 5, and 1 h contact time. The resulted solution was filtered , and the metal (Pb and Fe) concentrations in the filtrate were determined using AAS. This adsorption experiments were repeated 3 times.

The removal percentage of both Pb and Fe was determined using the equation below:

$$R\% = [(C_o - C_e)/C_o] \times 100 \quad (1)$$

C_o is the metal ion initial concentration (ppm), while C_e is the metal ion ultimate concentration (ppm).

The metal's adsorption capacity q_e(mg/g) was determined using the following equation:

$$q_e = C_o - C_e * (V/m) \quad (2)$$

V is the volume of the metal ion solution (L), and m is the mass of the adsorbent (g).

2.6.2. Batch Adsorption:

Batch adsorption experiments were proceeded using the peanutshell adsorbent (physically activated, chemical activated and physically-chemical activated) that finally exhibited the higher removal efficiency of Pb and Fe.

2.6.2.1. Adsorbent dosage:

To determine the impact of adsorbent dosage on the adsorption of Pb and Fe metal ion onto the sorbent material, Different adsorbent dosages (0.05, 0.1, 0.25, and 0.5 g) were combined with 25 mL of (50mg/L) metal ion solution. The mixture was kept at 30°C, with a pH of 5, and stirred for 60 minutes at 150 rpm. After filtration of the agitated solutions, the metal ions equilibrium concentration was estimated with an atomic absorption spectrophotometer (AAS)

2.6.2.2. Initial metal concentration:

0.25 g of adsorbent was mixed with 25 mL of different Pb and Fe metal concentrations (10, 30, 50, and 70 mg/l) as the initial , while maintaining the following other parameters: temperature (30°C), agitation speed (150 rpm), pH 5, and contact duration (60 minutes). The mixture was agitated and then filtered. The metal ions final concentration in the filtrate was estimated using AAS.

2.6.2.3. Contact time:

To examine the impact of different contact time on adsorption process, 0.25 g of the produced adsorbent was mixed with 25 ml of a 50 mg/L standard metal solution for different contact times (30, 45, 60, 75, and 90 minutes). The solutions were agitated at 150 rpm, with a constant pH 5 and a temperature 30°C. After the specified contact times, the samples were filtered and the metal ion equilibrium concentration was detected using AAS.

2.6.2.4. pH Effect :

The pH of the metal ion solution is a crucial factor in metal ion adsorption onto sorbents, as it influences the surface charge of the sorbent and the degree of ionization, thereby affecting the availability of binding sites (Liang et al, 2013; Javaid et al, 2011 ;Bansal et al, 2009). The impact of pH was evaluated across various values (2.5, 5, 7, 9). To do this, 0.25 g of the produced adsorbent was mixed with 25 mL of (50 mg /L) metal ion solution . After the solutions were shaken for 60 minutes at 150 rpm at room temperature, the aliquots were obtained by filtration and The metal ions equilibrium concentration in the filtrates was detected via AAS.

2.6.2.5. Temperature Effect:

Temperature effect on the metal adsorption was investigated at three different temperatures. A 0.25g of adsorbent was stirred with 25 mL of a metal ion solution (50 mg/L). The experiments were conducted at temperatures 303^{o}K, 323^{o}K, and 343^{o}K for 60 minutes, with a pH 5. After filtration, AAS was used to detect the metal ions final concentration in the solutions.

2.7.Adsorption isotherms:

2.7.1. Henry's isotherm model:

The Henry's isothermal model is a good fit for explaining the adsorption process at low concentrations, where adsorbate molecules do not interact with one another (Ayawei et al., 2017). This model assumes the concentrations in the adsorbent and solution phases to be connected by a linear expression, which can be expressed as:

$$q_e = K_{HE} C_e \qquad (3)$$

where q_e is the adsorption capacity at equilibrium (mg g^{-1}), K_{HE} is the Henry's equilibrium constant, and C_e is the metal ion equilibrium concentration in the solution (mg L^{-1}). Plotting Ce against qe yields a straight line, whose slope indicates the equilibrium constant K_{HE}.

2.7.2. Langmuir isotherm model:

According to the Langmuir isothermal model, adsorption takes place on a surface that has a limited number of identical sites., each of which can bind only one molecule of the adsorbate. This model assumes a homogeneous surface with no transmigration of adsorbate molecules across the surface and constant adsorption energy (Abdelsalam et al., 2011).

The linear form of the Langmuir model is

$$\frac{c_e}{q_e} = \frac{1}{Q_o\, b} + \frac{c_e}{q_e} \qquad \textbf{(4)}$$

where q_0 is the maximal adsorption capacity (mg g^{-1}) and b is the Langmuir constant (L mg^{-1}) (Kim et al 2015).

The slope and the intercept of the linear plot of Ce/qe vs Ce can be used to get the Langmuir constants q_o and b.

The separation factor, also known as the equilibrium parameter, or R_L, is a crucial Langmuir model parameter that determines the favorability or unfavorability of surfactant adsorption. Mathematically, it can be represented as

$$\mathbf{R_L} = \frac{1}{1 + b\, Q_o} \qquad \textbf{(5)}$$

where the Langmuir constant is denoted by b (dm^3/mg) and the highest initial concentration is represented by Q_o (mg/dm^3) (Prasath et al., 2014).

The isotherm's nature is shown by the parameter, R_L, as When $R_L < 1$, adsorption is generally considered favorable; when $R_L \sim 0$, adsorption is irreversible; when $R_L = 1$, the adsorption isotherm is linear; and when $R_L > 1$, unfavorable adsorption occurs.

2.7.3. Freundlich isotherm model:

This isotherm represents the balance between the quantity of adsorbate extracted per unit mass of the adsorbent and the concentration of adsorbate remaining in the solution (Sampranpiboon et al., 2014). This model takes into consideration the adsorbent surface's heterogenous character and assumes that the active sites and their energies are distributed exponentially. The linear equation of this model is:

$$\text{Log } q_e = \log k_F + \frac{1}{n} \log c_e \qquad (6)$$

The constant n in the Freundlich model is related to the efficiency of sorption and the energy of adsorption. K_F represents the adsorption capacity, By plotting log q_e against log C_e , a straight line with 1/n represents the slope and logK_F is the intercept was obtained. The value of K_F rises as the activated carbon's adsorption capacity does, suggesting a greater capacity to remove the adsorbate (Paudel and Shrestha, 2020). The range of 1/n values, which spans from 0 to 1, indicates how nonlinear the connection between adsorption and solution concentration is. The adsorption process is regarded as linear if 1/n = 1 (Ghasemi et al., 2016 & Kim et al., 2015). High values of n suggest a highly homogeneous surface , while low n values indicate significant adsorption at low solution concentrations. Additionally, a greater percentage of high-energy active sites is frequently indicated by low n values. (Arshadi et al., 2014).

2.7.4. Temkin isotherm model:

The Temkin isotherm model states that because of interactions between the adsorbent and adsorbate, the heat of adsorption falls linearly with increasing surface coverage (Obaid, 2020 ; Sampranpiboon et al., 2014). The Temkin model is expressed by the following equation:

$$Q_e = B\text{Ln}C_e + B\text{Ln}K_T \qquad (7)$$

In this equation, K_T (dm^3/g) represents the equilibrium binding constant, corresponding to the optimal binding energy, and B (J/mol) is a constant related to the heat of adsorption. (Edet & Ifelebuegu, 2020 & Javadian et al., 2015).

The constants B and K_T are determined By plotting of q_e versus ln(Ce) , where the slope and intercept represent B and ln(K_T), respectively.

2.7.5. Dubinin-Radushkevic (D-R) isotherm model:

This isotherm makes the assumption that the adsorbent's porosity and the characteristics of the adsorption curve are closely related (Sampranpiboon et al., 2014). It is especially helpful for calculating the apparent energy of adsorption and identifying the type of adsorption process, whether it is chemisorption or physisorption. The D-R model, unlike others, does not assume a homogeneous surface for the adsorbent (Edet and Ifelebuegu, 2020). This model is expressed as:

$$\ln q_e = \ln q_m - \beta E^2 \qquad (8)$$

In this equation, q_m is the adsorption capacity (mol/g), β is the Dubinin–Radushkevich constant (mol^2/KJ^2), and E is the adsorption energy, which can be expressed as :

$$E = RT \ln (1+1/C_e) \quad (9)$$

Where E is the polanyi potential, where C_e is the equilibrium concentration of the adsorbate ($mol.L^{-1}$), T is the absolute temperature (K) , and R is the universal gas constant ($8.314\times10-3$ KJ $mol-1K^{-1}$) .
The values of q_m , and B can be determined from the intercept and the slope , respectively of plotting ln qe vs E^2 . The following formula can be used to estimate the mean free energy E (kJ/mol) of sorption using B values:

$$E = 1/(2B)\ ½ \quad (10)$$

The type of adsorption is determined by the value of E; if E is greater than 16 kJ/mol, the adsorption is regarded as chemical; if E is less than 8 kJ/mol, the adsorption is regarded as physical.

2.8.**Adsorption kinetics:**

2.7.6. Pseudo first order (Largergren) kinetic model:

This model characterizes the rate of adsorbate removal over time as well as the rate of change in adsorbate uptake at a specific reaction time, which is exactly proportional to the difference between the equilibrium concentration and the concentration at time t. The following equation represents this model, which is also referred to as the Lagergren model (Edet and Ifelebuegu, 2020 & Santuraki and Muazu, 2015):

$$\text{Log } (q_e-q_t) = \log (q_e) - \frac{k_1}{2.303} t \quad (11)$$

Where: qe represents the adsorbent's adsorption capacity at equilibrium ($mg.g^{-1}$), q_t is the adsorbent's adsorption capacity at time t ($mg.g^{-1}$) and k_t represents the pseudo-first-order adsorption rate constant (min^{-1}).
Plotting log(qe−qt) against t produces a straight line, k_t and q_e can be determined from the slope and intercept, respectively.

2.7.7. Pseudo second order (PSO) kinetic model:

According to the Pseudo Second-Order (PSO) model , the rate of solute adsorption is directly proportional to the number of accessible sites on the adsorbent. According to (Ademiluyi and Nze, 2016), the equation used to describe the adsorption kinetics rate for the pseudo second-order model is:

$$\frac{t}{q_t} = \frac{1}{k_2\, qe^2} + \frac{1}{q_e}(t) \quad (12)$$

where q_e , q_t , and k_2 are the adsorption capacity at equilibrium ($mg.g^{-1}$), the adsorption capacity at time t ($mg•g^{-1}$), and the pseudo second-order adsorption rate constant ($gmg^{-1}min^{-1}$).
Plotting (t/q_t) in equation (12) against t yields a linear relationship. The values of q_e and k_2 can be ascertained from this plot's slope and intercept (Edet and Ifelebuegu, 2020).

2.7.8. Intra-particle diffusion (IP) kinetic model:

The Intraparticle Diffusion (IP) model has been extensively applied to determine the rate-limiting step during the adsorption process. Multiple phases of mass transfer, such as film diffusion,

surface diffusion, and pore diffusion, are involved in the adsorption of solutes from a solution. The IP model is typically studied using the Weber and Morris (1963) equation:

$$q_t = K_i\, t^{1/2} + C \qquad (13)$$

Where K_i is the rate constant (mg/g·min$^{0.5}$) and C is the boundary layer thickness. The influence of the boundary layer effect is shown by the value of C; larger values imply a more significant boundary layer effect. By plotting q_t against $t^{0.5}$ in equation (13) , a linear relationship is produced. If the line crosses the origin, it indicates that intraparticle diffusion (IP) is the controlling factor in the adsorption process. However, in many cases, the plot frequently shows several linear portions that each correspond to distinct mechanisms controlling the adsorption process rather than passing through the origin.

2.8. **Thermodynamic of adsorption:**

This model illustrates the link between temperature and the concentrations of the adsorbed metal ions onto the adsorbent at ideal contact time. Thermodynamic parameters such the change in standard Gibbs free energy (ΔG°), change in standard enthalpy (ΔH°), and change in standard entropy (ΔS°) were computed in order to evaluate the spontaneity of the adsorption process. The temperature was varied at 303, 323, and 343 °K, and the following equations were applied:

$$K_e = \frac{q_e}{c_e} \qquad (14)$$

$$\Delta G° = -RT \ln K \qquad (15)$$

$$\Delta G^0 = \Delta H^0 - T\Delta S^0 \qquad (16)$$

$$\ln K = -\frac{\Delta H^0}{RT} + \frac{\Delta S^0}{R} \qquad (17)$$

Where: ΔG° represents the change in standard free energy (kJ/mol), R is the universal gas constant (8.314 J/mol·K), K_e is the thermodynamic equilibrium constant, T is the absolute temperature in Kelvin.

By plotting lnKe versus 1/T , the values of ΔH° and ΔS° were determined from the slope and intercept of the plot . A positive ΔH° indicates that the adsorption process is endothermic, while a positive ΔS° reflects the affinity of the adsorbent for metal ions, suggesting an increase in sorbate concentration at the solid–liquid interface.

2.10. Regeneration tests:

This test is essential for determining the adsorbent's efficiency for multiple reuses. After the adsorption process, the metal-laden adsorbent was first cleaned with 0.1M HCl to get rid of any remaining or loosely attached metal ions from its surface. After that, it was dried overnight in an oven at 60°C .

Batch adsorption experiments were conducted repeatedly until equilibrium was achieved. The concentrations of metal ions were measured using an Atomic Absorption Spectrophotometer (AAS) immediately after filtration.

2.11. Application in real water sample:

The adsorption rates of heavy metals by the prepared adsorbent was evaluated using two real water samples from Lake Nasser: one collected from Aswan, Egypt, and the other from Wadi Halfa, Sudan. The Aswan sample was gathered near the Lake Nasser Development Organization, while the Sudanese sample was collected from a port in Sudan. For the assessment, a known quantity of heavy metal was introduced into 25 mL of each real water sample . Adsorbent dose,

temperature, pH, and starting metal ion concentration were all tuned during the experiment. Following this, the samples were shaken for a preset ideal contact time at 150 rpm. Using an atomic absorption spectrophotometer (AAS), the amount of metal ions remained in the solution were determined after the solutions had been shaken and filtered.

3. Results and Discussion

3.1. Comparative study of different prepared adsorbents for Pb and Fe adsorption :

The adsorption efficiency of Pb and Fe ions by the prepared peanut shell adsorbents at constant 0.25g adsorbent dosage , 50 mg/L metal ion solution, 1 hour of shaking, pH 5, and 30°C showed that $PS_{800,NaOH}$ adsorbent show higher percentage removal of Pb and Fe ions (99.76% and 99.94%), respectively than the other adsorbents (Tables 1 and 2) . As a result, This adsorbent, known as $PS_{800,NaOH}$, was thus chosen for additional batch adsorption investigations.

Table. 1 the adsorption removal percentage of Pb using peanut shell biosorbent.

Sample	R%
1- Physically prepared adsorbent	
Ps_{300}	98.4
Ps_{500}	98.2
Ps_{800}	98.8
2- Chemically prepared adsorbent	
Ps_{Hcl}	45.4
Ps_{H3PO4}	42.8
Ps_{NaOH}	66.8
3- Physically followed by chemically prepared adsorbent	
$Ps_{300,Hcl}$	40.2
$Ps_{300,H3PO4}$	37.6
$Ps_{300,NaOH}$	99.4
$Ps_{500,Ccl}$	54.8
$Ps_{500,H3PO4}$	58.0
$Ps_{500,NaOH}$	95.8
$Ps_{800,HCl}$	52.6
$Ps_{800,H3PO4}$	87.4
$Ps_{800,NaOH}$	99.76

Table.2 The adsorption removal percentage of Fe using peanut shell adsorbent.

Sample	R%
1- Physically prepared adsorbent	
Ps_{300}	58.8
Ps_{500}	70
Ps_{800}	70.2
2- Chemically prepared adsorbent	
Ps_{Hcl}	59.44
Ps_{H3PO4}	57.52
ps_{NaOH}	60.8
3- Physically followed by chemically prepared adsorbent	
$Ps_{300,Hcl}$	54.3
$Ps_{300,H3PO4}$	55.5
$Ps_{300,NaOH}$	79.2
$Ps_{500,Hcl}$	53.8
$Ps_{500,H3PO4}$	54.4
$Ps_{500,NaOH}$	98.44
$Ps_{800,Hcl}$	54.6
$Ps_{800,H3PO4}$	54.4
$Ps_{800,NaOH}$	99.94

3.2. Characterization of peanut shell adsorbent:

SEM images of the prepared peanut shell biochar ($PS_{800, NaOH}$) were illustrated in Fig. (1). a more irregular, rigid, rough surface with a porous structure was apparent in contrast to the inactivated peanut shell. The peanut shell biochar ($PS_{800, NaOH}$) enhanced the development of the porous structure that enable it to stimulate diffusion of the metal ions onto active sites of the adsorbent surface (Dotto et al., 2014). Raising the carbonization temperature contributed significantly to the creation of cleaner and smoother pore sizes by totally eliminating the residues produced by the carbonization process .

From EDX results of peanut shell biochar ($PS_{800, NaOH}$) in Fig. (2), it was observed that , the oxygen content increased from 35.04 for (the natural sample) to 53.52% for the peanut shell biochar .

Fig. (3) displayed the activated peanut shell's FTIR spectrum. The large peak at 3427.8 cm^{-1} was ascribed to the stretching vibrations of the O-H groups with intramolecular hydrogen bonds of the cellulose stretching (Huo et al., 2013). Iqbal et al. (2009) claimed that the C–H stretching vibration of alkyl compounds was responsible for the band at 2923.5 cm^{-1}. The band at 1630 cm^{-1} indicates the C=O stretching of carboxylic acid in hemicelluloses, lignin, or pectin. The

peak at 1404 cm^{-1} represents the C–C stretching vibration. It was determined that the peak at 1048.3 cm^{-1} was caused by stretching C–O bonds in ethers or alcohols. The C–H stretching vibration was attributed to the peaks at 668.5 cm^{-1} .

according to the X-ray diffraction (XRD) analysis of peanutshell biochar chemically treated with NaOH ($PS_{800,\ NaOH}$), that was depicted in Fig. 4, The activated peanut shell biochar has an amorphous phase for hemicelluloses, lignin, and pectin . The peanut shell's maxima at 22.4°, 24.4°, 30.6°, and 31.8° 2θ show that cellulose makes up the majority of its composition. The only substance with a crystalline phase is cellulose.

Table 3 displayed the activated peanut shell's textural characteristics. When compared to the unactivated peanut shell, it is evident that the prepared peanut shell biochar had a higher BET value as well as micropores volume and total pore volume. The peanut shell is an effective adsorbent because of its porosity, which encourages the binding of metal ions onto its available active sites.

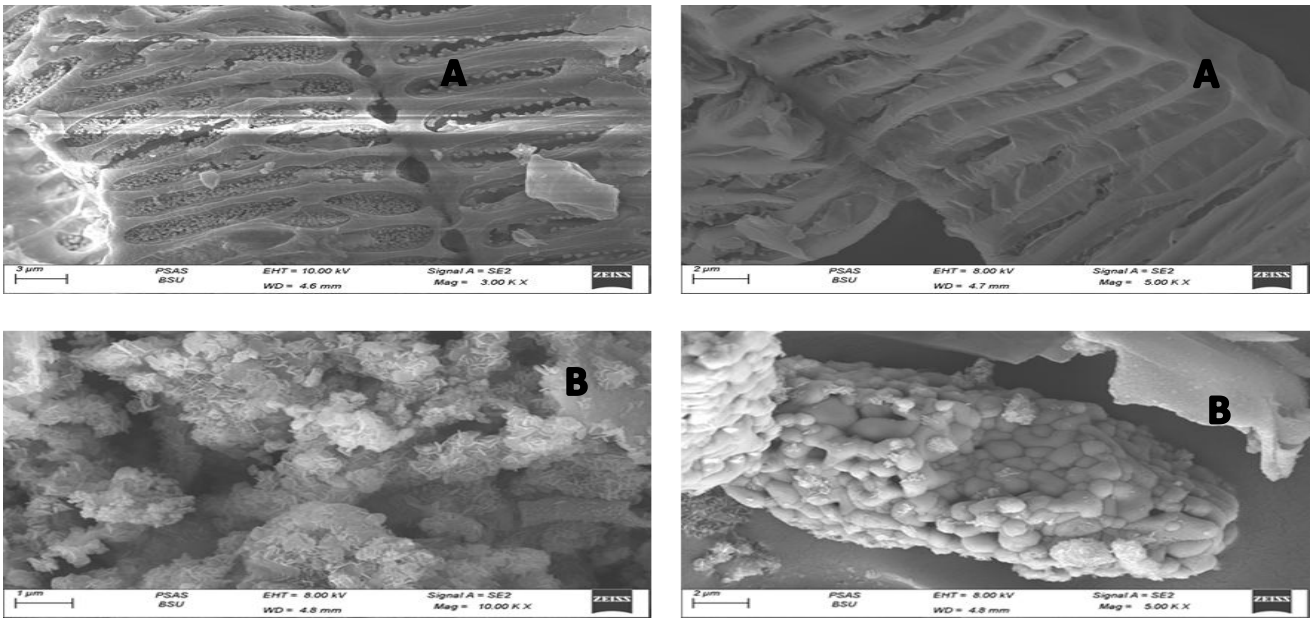

Fig. 1 SEM image of (A) the untreated peanutshell; (b) activated peanut shell biochar ($PS_{800,\ NaOH}$)

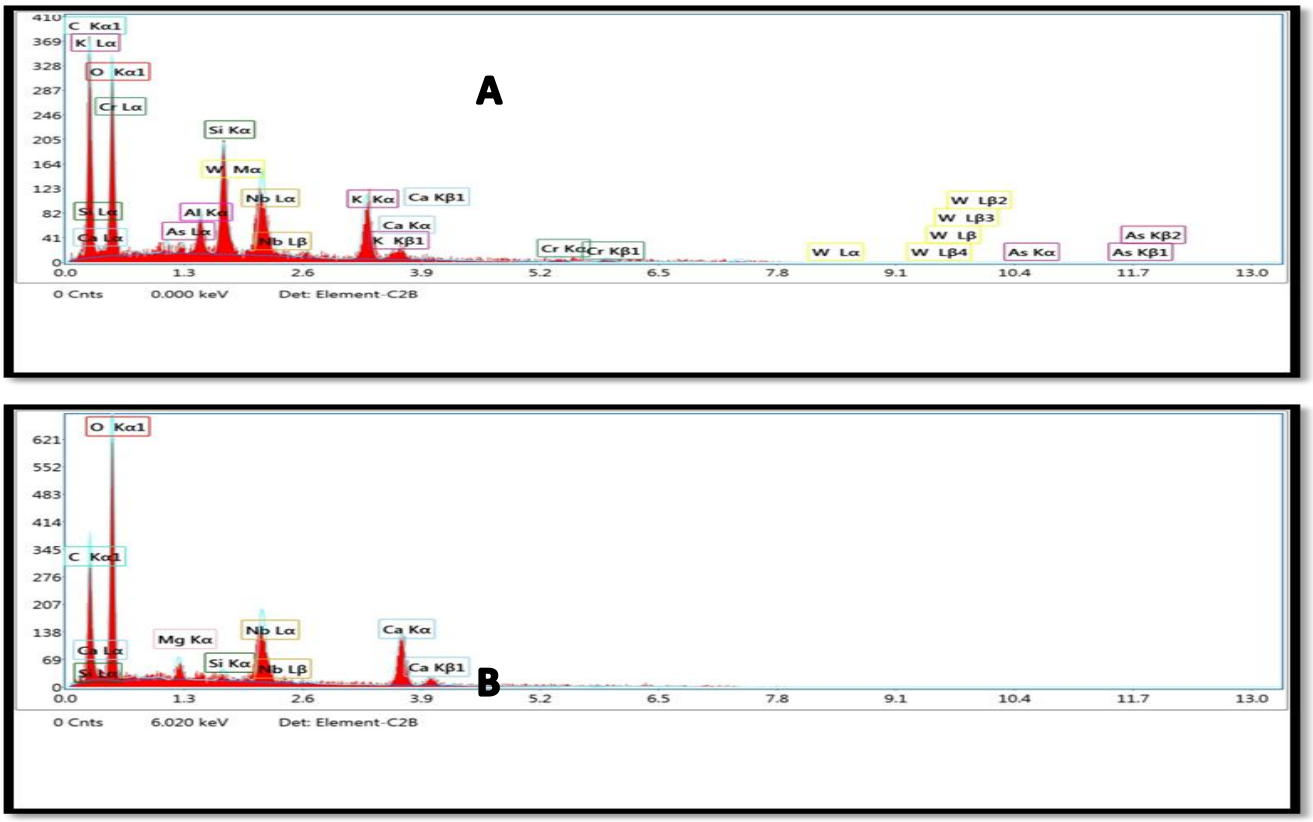

Fig.2 EDX image of (A) the untreated peanut shell; (B) activated peanut shell biochar ($PS_{800, NaOH}$)

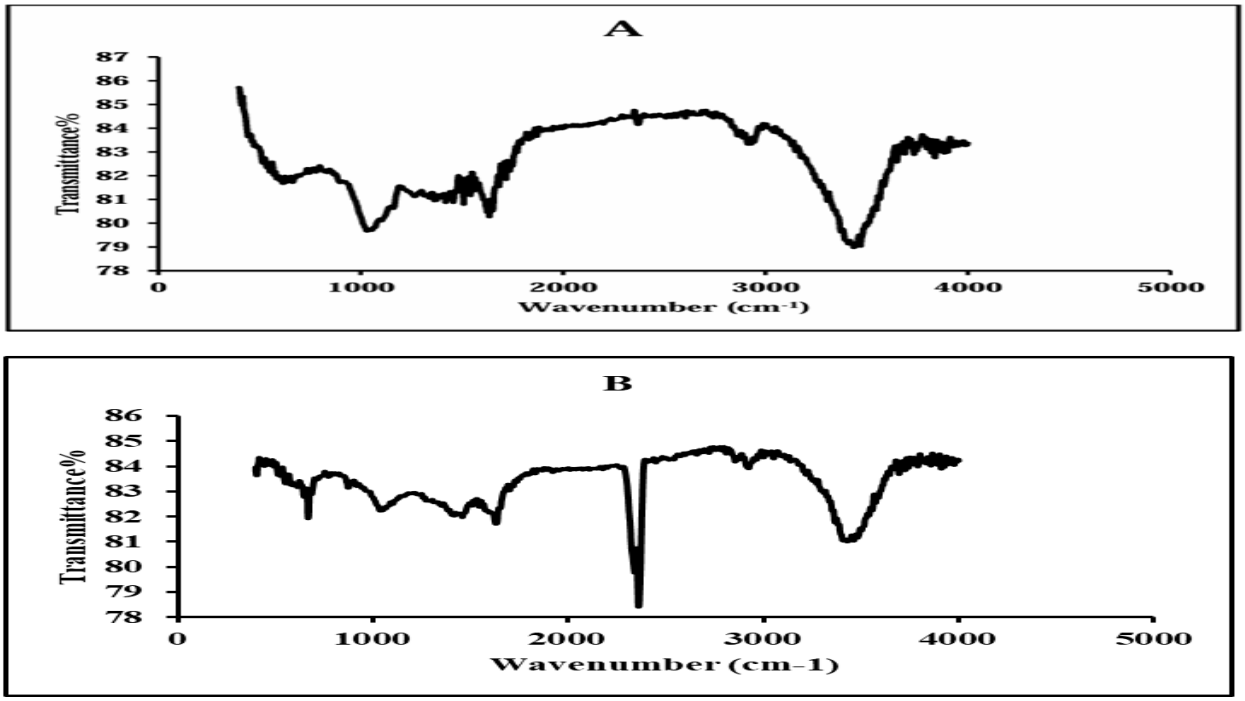

Fig. 3 FTIR spectra of (A) the untreated peanutshell ; (B) activated peanut shell biochar ($PS_{800, NaOH}$)

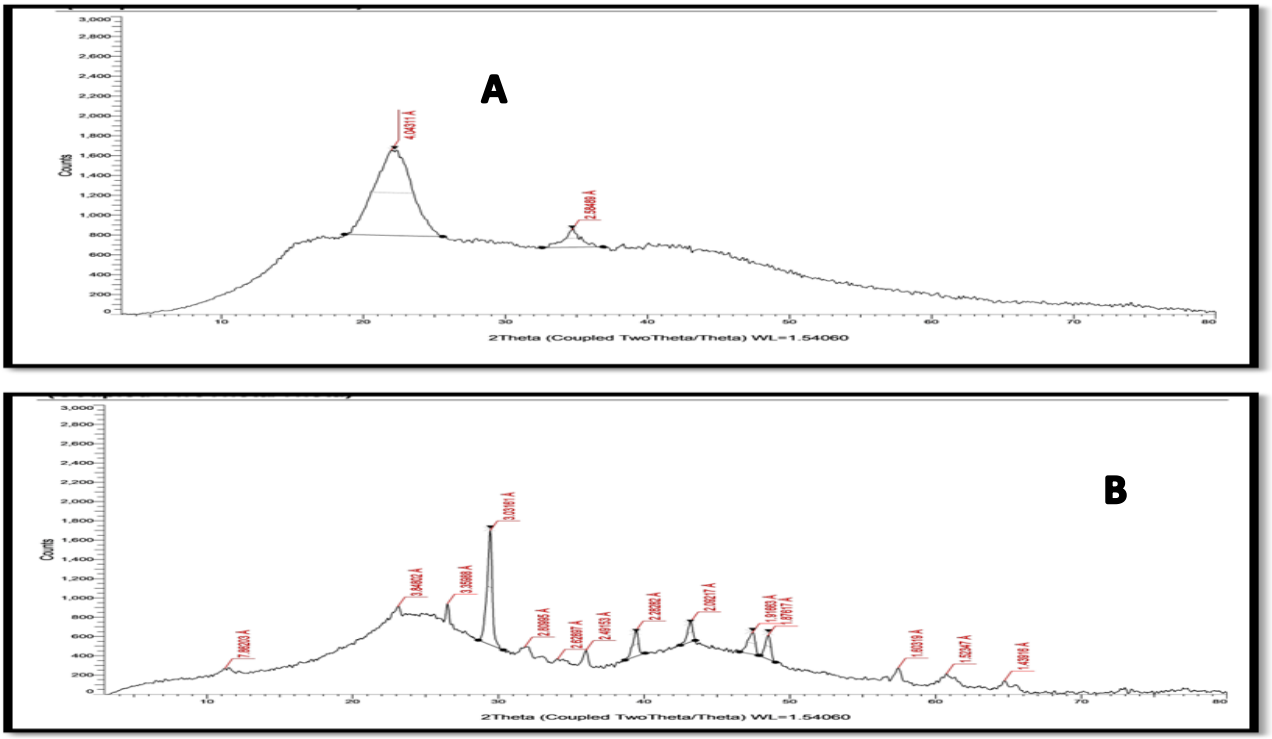

Fig. 4 XRD analysis of (A) the untreated peanutshell ; (B) activated peanut shell biochar ($PS_{800, NaOH}$)

Table 3. Textural properties of the activated peanut shells

Sample	Surface area (m^2/g)	Pore volume (cm^3/g)	Average pore radius (nm)
the untreated peanutshell	2.08	0.007	7.515
activated peanutshell biochar ($PS_{800, NaOH}$)	44.15	0.049	2.225

3.3. Optimum parameters for the adorption of Pb and Fe on peanutshell adsorbent ($PS_{800, NaOH}$):

3.3.1. Effect of adsorbent dose:

The number of accessible active sites on the adsorbent surface is determined by the amount of adsorbent (Maki and Qasim, 2023). Because of this, the effects of the activated peanut shell dosage were investigated by altering the dosage (0.05, 0.1, 0.25, and 0.5g) at set initial metal ion concentration of (50 mg/L) , pH (5) and contact duration (60 min). Figure (5) show the removal effectiveness of the various adsorbent dosages. According to the Pb adsorption data, 0.5 g of activated peanut shell produced the best removal percentage (99.88%). This outcome is explained by the fact that as the adsorbent dosage increases, so do the possible active binding sites (Garg et al., 2019). However, for Fe, the increase in metal ion-covered active sites leading to a loading in the adsorbent capacity is responsible for the decrease in removal effectiveness with adsorbent doses greater than 0.1 g (Maki and Qasim, 2023).

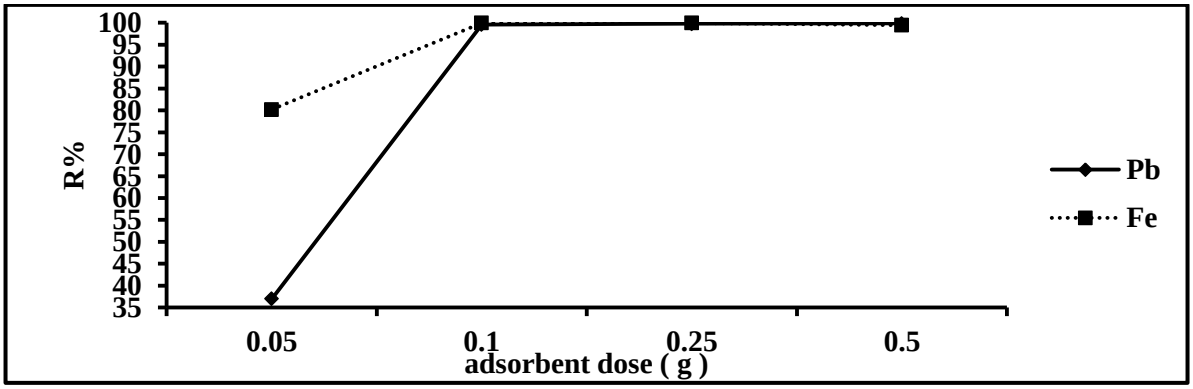

Fig. 5 .Removal of Pb and Fe ions on peanutshell adsorbent ($PS_{800,\ NaOH}$) according to adsorbent dose.

3.3.2. Iinitial metal ion concentration:

Figure (6) present the data about the impacts of various metal ion (Pb and Fe) concentrations (10, 30, 50, and 70 mg/L) on the adsorption efficiency of the prepared activated peanut shell biochar ($PS_{800,\ NaOH}$) . The obtained results demonstrated that at the metal concentrations of 50 mg/l, the removal efficiency for the examined metal ions, Pb and Fe, on the peanut shell adsorbent, reached its maximum (99.85 , 99.94%) ,respectively. This implies the adsorption efficacy increased slightly in tandem with the metal content.This is because the metal ion molecules were present at higher concentrations and hense occupied more active binding sites (Georgin et al., 2016).

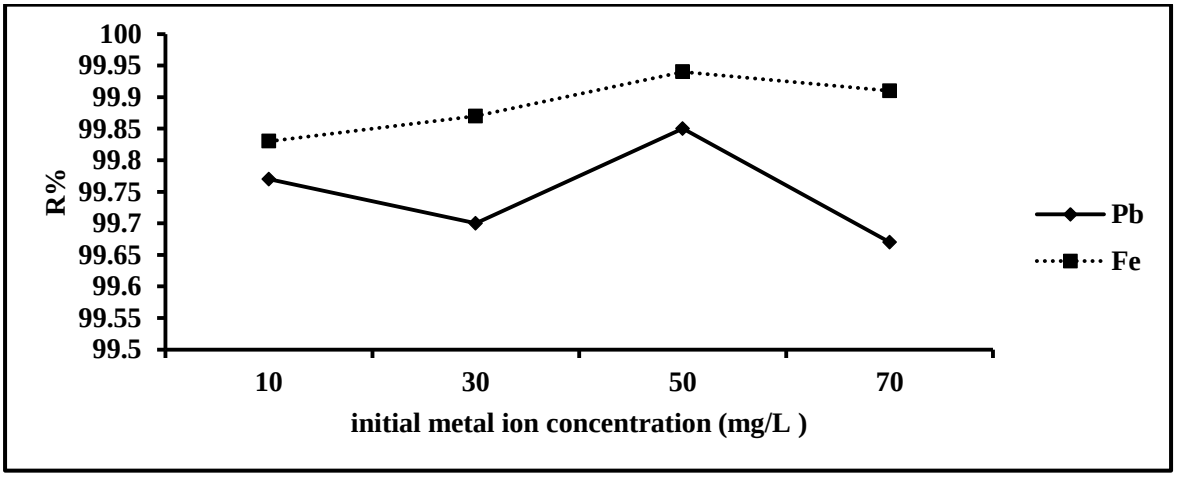

Fig.6. Removal of Pb and Fe ions on peanutshell adsorbent ($PS_{800,\ NaOH}$) according to initial metal ion concentration.

3.3.3. Contact time:

Figure 7 displays the data gathered from the removal of the metal ions under study by the prepared activated peanut shell biochar at different contact durations (30–90 min) and optimal pH. Results demonstrated that the adsorption capacity of lead in the solution decrease from the maximum 99.80% to 99.72% when contact time increases from 30 min to 90 min. As there are several active sites available to increase the proportion of metal ions removed from the adsorbent surface, it is possible that the removal of the examined metal ion, lead (Pb), occurred quickly

within the first half hour (Abo El-Enein et al., 2017). On the other hand, when the contact time increased from 30 to 90 minutes, the number of uncovered surface areas and remaining active sites decreased. (Maki and Qasim, 2023). Consequently, based on the data acquired , 30minutes of contact time was found to be the optimal duration for achieving the highest level of lead adsorption (up to 99.8% elimination) on the surface of activated peanutshell. The adsorption capacity of peanutshell shell adsorbent ($PS_{800,\ NaOH}$) towards Fe was found to be directly proportional to time, the iron removal efficiency from the solution increased slightly with increasing time, from 99.934% to its optimum (99.986%) at 90 min.

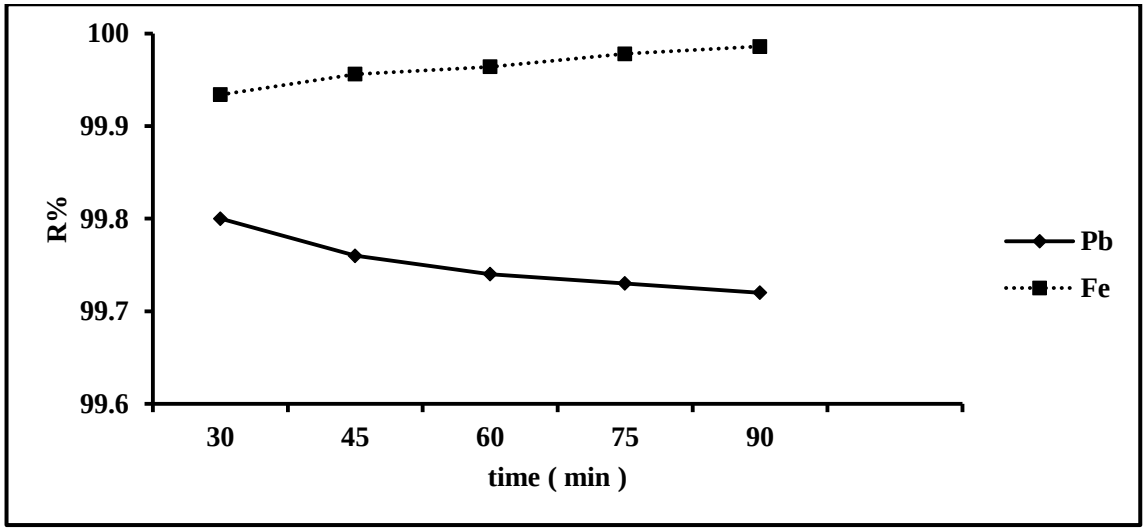

Fig.7. Removal of Pb and Fe ions on peanutshell adsorbent ($PS_{800,\ NaOH}$) according to contact time.

3.3.4. pH Effect:

The adsorption capability of peanut shell biochar was assessed at pH levels of 2.5, 5, 7, and 9,.The temperature was 30°C throughout the procedure, with the adsorbent dosage set at 0.25 g/25ml, the starting metal ion concentration at 50 mg / L, and a fixed contact time of 60 minutes. It is evident that raising the solution pH from 2.5 to 5 increased the percentage of metal ions (Pb and Fe) removed. At pH 5, the greatest values of 99.84% and 99.98% for the removal of Pb and Fe , respectively were attained. After then, The efficiency of adsorption for the removal of metal ions decreased as the pH level rose. At lower pH value (2.5),the concentration of protons present on the surface of the peanut shell is known to rise, This, in turn, increases the competition between protons and metal ions for the available active binding sites on the peanut shell surface, and hense increases the amount of free metal ions that are left in the solution (Witek-Krowiak et al., 2011). However, when pH rises, the hydroxyl anion causes the metal ions to precipitate and increase in the solution, which lowers the percentage of removal for both heavy metals (Pb and Fe) (Aryee et al., 2021). Consequently, pH 5 is the ideal pH to remove Pb and Fe ions from solutions.

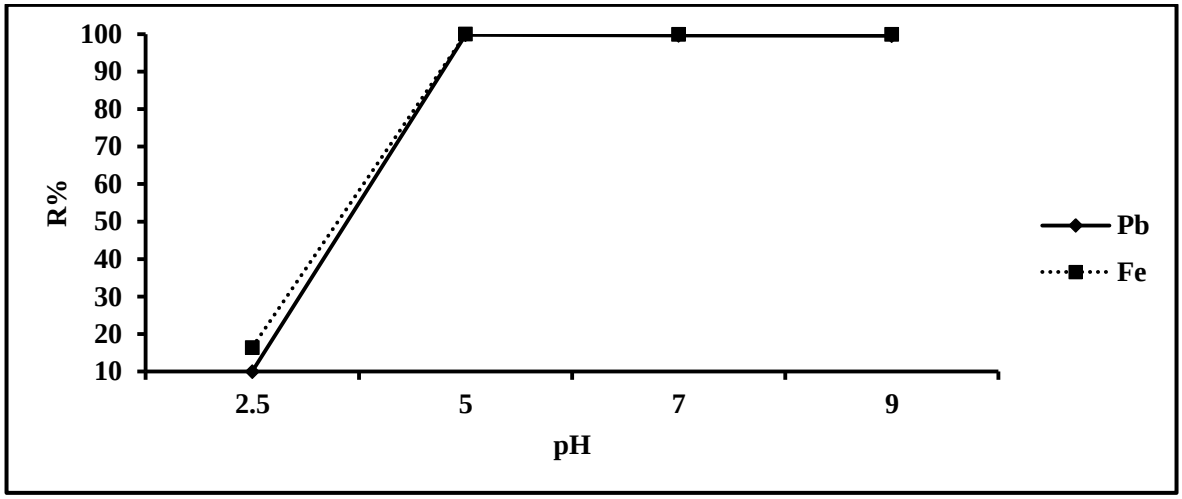

Fig.8. Removal of Pb and Fe ions on peanutshell adsorbent ($PS_{800, NaOH}$) according to pH.

3.3.5. Effect of temperature:

Figure (9) show the impact of various temperature parameters (303, 323, and 343 K) on the percentage of metal ions (Pb and Fe) removed by the prepared activated peanut shell biochar under optimal experimental conditions. As the temperature rises from 303 to 323 K , the lead removal percentage was raised to a maximum of 99.99% at 323 K, after which it gradually dropped. The weak adsorptive interactions between the active sites and metal ions on the surface of the peanut shell can be the cause of the drop in the proportion of metal ions removed when the temperature rises over 323 K. On the other hand, (Isawi, 2020) stated that a rise in temperature would cause the solution to become more viscous, which will lead to a decrease in the movement of metal ions and ultimately a reduction in the efficiency of adsorption. The optimal temperature for removing Fe ions from biochar was determined to be 303 K, as the removal percentage of Fe decrease after this point. Based on the results, 323 K was determined to be the optimal temperature for lead adsorption and 303 K for iron adsorption.

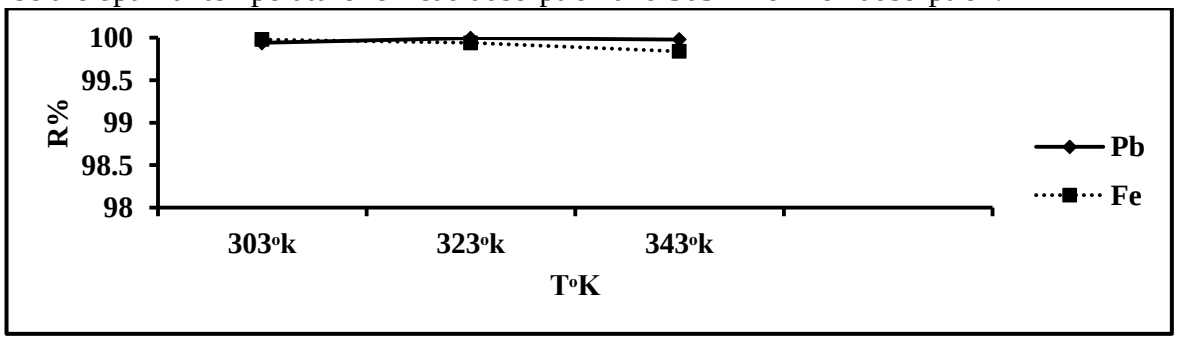

Fig. 9 Removal percentage of Pb and Fe ions on peanutshell biosorbent ($PS_{800, NaOH}$) according to temperature.

3.4. Adsorption isotherms:

3.4.1. Henry's Isotherm:

According to the data illustrated in Table (4) , the K_{HE} derived from the slope was 33.5 and 109.67 for lead and iron, respectively. This result showed that Fe ions had a higher equilibrium distribution on the adsorbent surface than Pb ions did.

3.4.2. Langmuir Isotherm:

The obtained R_L values were 0.022 and 0.0013 for Pb and Fe ions, respectively, based on the Langmuir isotherm parameters displayed in Table (4) . As was noted, the Langmuir isotherm is favorable for this investigation as the value of R_L fell between 0 and 1. Pb and Fe have respective R^2 values of 0.63, 0.56, b values of 2.1, 213.6, and Qo values of 21.55, 3.6. These data made it evident that Pb has a larger maximum adsorption capacity (Qo) than Fe, and as a result, the adsorbent has a stronger affinity for Pb ions when it comes to adsorption.

Table. 4 Adsorption isotherms calculated parameters for the adsorption of Pb and Fe on peanutshell biosorbent.

parameter	Pb	Fe
Henry isotherm model		
K_{HE} (L g^{-1})	33.5	109.67
R^2	0.89	0.7
Langmuir isotherm model		
Q_o	21.55	3.6
B_L (L /mg)	2.1	213.6
R_L	0.022	0.0013
R^2	0.63	0.56
Freundlich isotherm model		
1 /n	0.87	0.97
K_f ($mg^{-1/n} L^{1/n} g^{-1}$)	27.7	72.4
R^2	0.94	0.26
Temkin isotherm model		
B (J /mol)	2.5877	3.99
K_f (L /G)	56.41	83.19
R^2	0.89	0.7
Dubinin – Raduskevich isotherm model		
Q_D (mg /g)	10.518	34.4
E (kj /mol)	4.0825	4.0825
B (mol^2/kj^2)	3×10^{-8}	3×10^{-8}
R^2	0.96	0.74

3.4.3. Freundlich isotherm

The Freundlich isotherm results are recorded in Table (4). The results reveal that 1 /n = 0.87 and 0.97 for Pb and Fe, respectively, indicating the favorability of Pb and Fe ions adsorption on the produced adsorbent. Based on the data presented in Table (4), the K_f values for Pb and Fe were 27.7 and 72.4, respectively. According to this concept, the larger value of K_f indicates the higher affinity for the adsorption of Fe ions' on the adsorbent surface than for Pb ions. The Langmuir isotherm model offered the best correlation of the experimental data of Fe ions, as demonstrated by the value of R^2, while Freundlich isotherm model, on the other hand, provides the most accurate description of Pb ion adsorption on the produced adsorbent.

3.4.4. Temkin isotherm:

Table (4) provided the values of B and K for the temkin isotherm. For Pb and Fe, the values of B were 2.58, and 3.99, respectively. This finding suggests that Pb ions have a lower heat of adsorption than Fe ions.

3.4.5. Dubinin-Radushkevich isotherm (D-R):

The values of E = 4.08 for both Pb and Fe can be found in Table (4) . Since E is less than 8, this model regarded Pb and Fe ions adsorption as physical adsorption.

3.5. Adsorption kinetic Studies:

3.5.1. Pseudo-First-Order (Lagergren) kinetic Model:

Table (5) show the findings of Pb and Fe adsorption kinetic tests on peanutshell. The K_1 (min^{-1}) values for Pb and Fe were -0.0091 and 0.0342, respectively. The kinetic mechanism of adsorption could not be expressed by the first order model since the estimated q_e did not approach the value of the experimental q_e. For the peanutshell adsorbent ($PS_{800,\ NaOH}$), the correlation coefficient (R^2) for Pb and Fe was 0.77 and 0.88, respectively.

3.5.2. Pseudo second order Model:

Based on the data in Table (5), the computed values of q_e for Pb and Fe were 4.98 and 5, respectively, and they were almost the same as the experimental value of q_e. The k_2 values for Pb and Fe were 2.5 and 0.7, respectively. As demonstrated by the R^2 result being higher for pseudo second order than pseudo first order, the pseudo second order model was better suited for the adsorption of both heavy metals, Pb and Fe, on the produced peanutshell adsorbent.

3.5.3. Intra-Particle Diffusion Model

According to the obtained data in Table (5) , the C values of Pb and Fe ions were 1.9946 and 4.9929, respectively. The significant contribution of diffusion within particles during Pb and Fe ion adsorption was suggested by the high correlation coefficients for Pb and Fe, which were 0.87 and 0.99 .It was clear that there was border and intraparticle diffusion, and the plateau supported the several steps that influence the adsorption process. The connection between q_t and $t^{0.5}$ was also not linear across the whole time range.

Table. 5 Calculated kinetic parameters for the adsorption of Pb and Fe on peanut shell adsorbent ($PS_{800, NaOH}$).

parameter	Pb	Fe
Pseudo first order model		
K_1 (min^{-1})	-0.0091	0.0342
$q_{e\ (\ calculated\ )}$ (mg/g)	0.0017	0.0006
R^2	0.77	0.88
Pseudo second order model		
K_2	2.5	0.7
$q_{e\ (\ calculated\ )}$ (mg/g)	4.98	5
$q_{e\ (\ experimental\ )}$ (mg/g)	4.99	4.9991
R^2	1	1
Intra particle diffusion model		
K_{ip}	-0.0009	0.0007
C (mg/g)	1.9946	4.9929
R^2	0.87	0.99

3.6. Thermodynamics of adsorption:

The positive values of ΔH° (44.9 and 94.2) for Pb and Fe in Table (6) data show that adsorption is of endothermic nature. The negative values of ΔS° demonstrated less randomness at the solid/solution interface, whereas the negative values of ΔG° for all applied temperatures suggested a spontaneous adsorption process.

Table.6 Thermodynamic model parameters for the adsorption of Pb and Fe ions on peanut shell adsorbent ($PS_{800,NaOH}$).

parameter		Pb	Fe
ΔH^o, kj /mol		44.86	94.15
ΔS^o, kj /mol K		-.0964	-0.25
ΔG^o, kj /mol	303	-12.898	-15.6
	323	-21.5	-13.7
	343	-17.7	-11.9
R^2		1	0.83

3.7. Regeneration test:

The regeneration efficiency of five cycles of Pb ions was 99.96, 99.948, 99.87, 99.84, and 99.84%, as shown in Fig (10) , whereas the corresponding values for Fe ions were 99.88, 56.6, 59.8, 58.4, and 58.4%. It was shown that for Fe, the regeneration efficiency clearly decreased as the number of cycles increased. Therefore, up to five cycles, the Pb ion adsorption efficiency on peanut shell adsorbents was better than Fe.

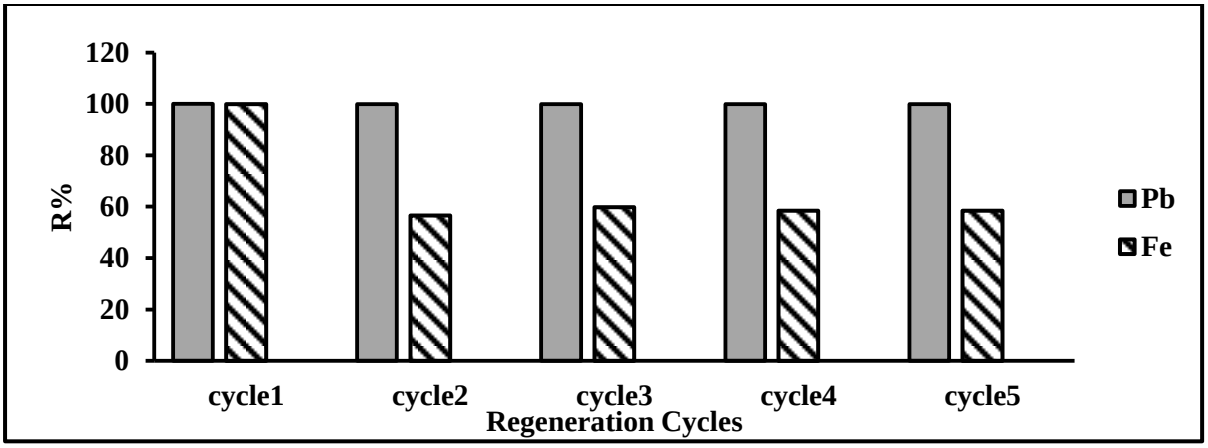

Fig. 10 Regeneration removal percentage of Pb and Fe ions on peanutshell adsorbent ($PS_{800,\ NaOH}$).

3.8. Application on real water samples:

Concentration of lead in the real water samples from Egypt and Sudan was 0.03mg/l, while that for iron was 0.03and 0.02mg/l in Egypt and Sudan, respectively. The concentration of Pb and Fe was adjusted to the optimum (50mg/l) . Figure (11) show that Pb and Fe ions removal percentage surpasses 99%, demonstrating the efficacy of the produced adsorbent in purifying Lake Nasser water.

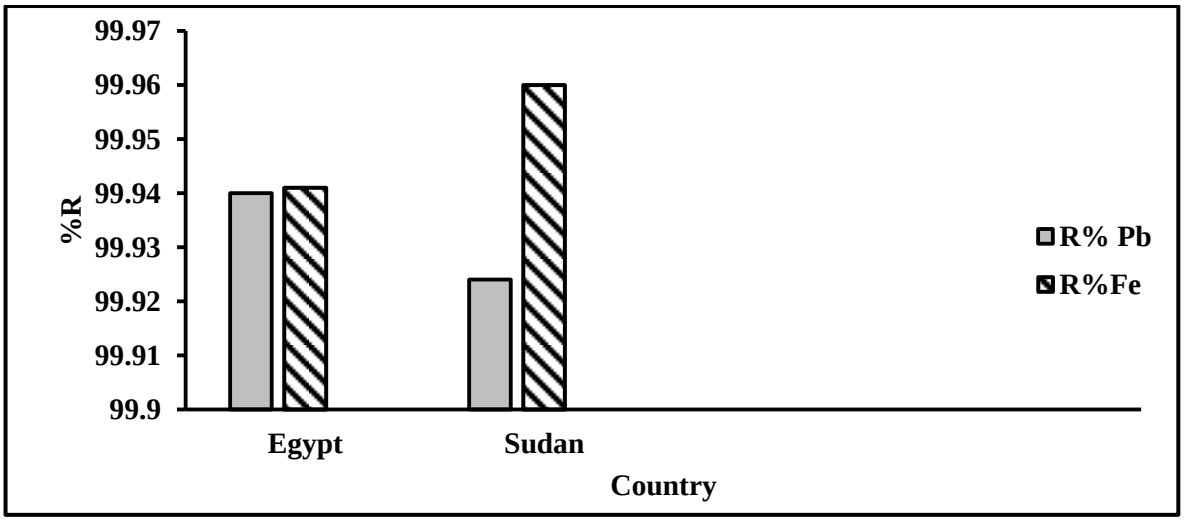

Fig.11 Adsorption removal percentage of Pb and Fe ions of the real water samples from Lake Nasser (Egypt and Sudan part) on peanut shell adsorbent (PS800, NaOH).

Conclusion

This study examined the capacity of several prepared peanut shell sorbents to remove iron and lead from water. According to the results, $PS_{800,NaOH}$ has the greatest capacity to remove both heavy metals because of its vast surface , rich and diverse functional groups. Pb and Fe adsorption fit the Freundlich and Langmuir isotherms, respectively and the (PSO) kinetic model for adsorption. The adsorption of both heavy metals was endothermic and spontaneous. The notable amount of Pb and Fe removed from Lake Nasser showed that peanut shell biochar has the potential to be an economical, safe, and ecologically friendly sorbent.

References:

AbdelSalam, O.E.; Reiad, N.A. and ElShafei, M.M. (2011). A study of the removal characteristics of heavy metals from wastewater by low-cost adsorbents. Journal of Advanced Research, 2(4), 297-303.

Abo-El-Enein, S.A.; Shebl, A. and El-Dahab, S.A. (2017). Drinking water treatment sludge as an efficient adsorbent for heavy metals removal. Applied Clay Science, 146, 343-349.

Ademiluyi,T, F. and Nze, C.J. (2016). Sorption characteristics for multiple adsorption of heavy metal ions using activated carbon from Nigerian bamboo. Journal of Materials Science and Chemical Engineering, 4(4), 39-48.

Arshadi, M.; Amiri, M.J. and Mousavi, S. (2014). Kinetic, equilibrium and thermodynamic investigations of Ni (II), Cd (II), Cu (II) and Co (II) adsorption on barley straw ash. Water resources and industry, 6, 1-17.

Aryee, A.A.; Mpatani, F.M.; Du, Y.; Kani, A.N.; Dovi, E.; Han, R.; ... and Qu, L. (2021). Fe3O4 and iminodiacetic acid modified peanut husk as a novel adsorbent for the uptake of Cu (II) and Pb (II) in aqueous solution: characterization, equilibrium Pollution, 268, 115729.

Ayawei, N.; Ebelegi, A.N. and Wankasi, D. (2017). Modelling and interpretation of adsorption isotherms. Journal of chemistry, 2017(1), 3039817.

Bansal, M.; Singh, D. and Garg, V.K. (2009). A comparative study for the removal of hexavalent chromium from aqueous solution by agriculture wastes' carbons. Journal of hazardous materials, 171(1-3), 83-92.

Barakat, M.A. (2011). New trends in removing heavy metals from industrial wastewater. Arabian journal of chemistry, 4(4), 361-377.

Bello, O.S.; Bello, I.A. and Adegoke, K.A. (2013). Adsorption of dyes using different types of sand: A review. South African Journal of Chemistry, 66, 117-129.

Carolin, C.F.; Kumar, P.S.; Saravanan, A.; Joshiba, G.J. and Naushad, M. (2017). Efficient techniques for the removal of toxic heavy metals from aquatic environment: A review. Journal of environmental chemical engineering, 5(3), 2782-2799.

Demirbas, A. (2008). Heavy metal adsorption onto agro-based waste materials: a review. Journal of hazardous materials, 157(2-3), 220-229.

Dotto, G.L.; Buriol, C. and Pinto, L.A.D.A. (2014). Diffusional mass transfer model for the adsorption of food dyes on chitosan films. Chemical Engineering Research and Design, 92(11), 2324-2332.

Edet, U.A. and Ifelebuegu, A.O. (2020). Kinetics, isotherms and thermodynamic modeling of the adsorption of phosphates from model wastewater using recycled brick waste. Processes, 8(6), 665.

Ewecharoen, A.; Thiravetyan, P.; Wendel, E. and Bertagnolli, H. (2009). Nickel adsorption by sodium polyacrylate-grafted activated carbon. Journal of hazardous materials, 171(1-3), 335-339.

Garg, D.; Kumar, S.; Sharma, K. and Majumder, C.B. (2019). Application of waste peanut shells to form activated carbon and its utilization for the removal of Acid Yellow 36 from wastewater. Groundwater for Sustainable Development, 8, 512-519.

Georgin, J.; Dotto, G.L.; Mazutti, M.A. and Foletto, E.L. (2016). Preparation of activated carbon from peanut shell by conventional pyrolysis and microwave irradiation-pyrolysis to remove organic dyes from aqueous solutions. Journal of Environmental Chemical Engineering, 4(1), 266-275.

Ghasemi, M.; Javadian, H.; Ghasemi, N.; Agarwal, S. and Gupta, V.K. (2016). Microporous nanocrystalline NaA zeolite prepared by microwave assisted hydrothermal method and determination of kinetic, isotherm and thermodynamic parameters of the batch sorption of Ni (II). Journal of Molecular Liquids, 215, 161-169.

Huo, S.; Ulven, C.A.; Wang, H.; Wang, X. (2013). Chemical and mechanical properties studies of chi-composites. Polymers and Polymer Composites, 21(5), 275–28

Husaini, S.; Zaidi, J.; Matiullah and Akram, M. (2011). Evaluation of toxic metals in the industrial effluents and their segregation through peanut husk fence for pollution abatement. Journal of Radioanalytical and Nuclear Chemistry, 289(1), 203-211.

Hussain, A.; Madan, S. and Madan, R. (2021). Removal of heavy metals from wastewater by adsorption. Heavy metals—Their environmental impacts and mitigation.

Isawi, H. (2020). Using zeolite/polyvinyl alcohol/sodium alginate nanocomposite beads for removal of some heavy metals from wastewater. Arabian Journal of Chemistry, 13(6), 5691-5716.

Javadian, H.; Ghorbani, F.; Tayebi, H.A. and Asl, S.H. (2015). Study of the adsorption of Cd (II) from aqueous solution using zeolite-based geopolymer, synthesized from coal fly ash; kinetic, isotherm and thermodynamic studies. Arabian Journal of Chemistry, 8(6), 837-849.

Javaid, A.; Bajwa, R.; Shafique, U. and Anwar, J. (2011). Removal of heavy metals by adsorption on Pleurotus ostreatus. Biomass and Bioenergy, 35(5), 1675-1682.

Kılıç, Z. (2020). The importance of water and conscious use of water. International Journal of Hydrology, 4(5), 239-241.

Kim, N.; Park, M. and Park, D. (2015). A new efficient forest biowaste as biosorbent for removal of cationic heavy metals. Bioresource technology, 175, 629-632.

Ledezma, C.; Negrete-Bolagay, D.; Figueroa, F.; Zamora-Ledezma, E.; Ni, M.; Alexis, F. and Guerrero, V.H. (2021). Heavy metal water pollution: A fresh look about hazards, novel and conventional remediation methods. Environmental Technology and Innovation, 22, 101504.

Liang, F.B.; Song, Y.L.; Huang, C.P.; Li, Y.X. and Chen, B.H. (2013). Synthesis of novel lignin-based ion-exchange resin and its utilization in heavy metals removal. Industrial and Engineering Chemistry Research, 52(3), 1267 1274.

Madhubashani, A.M.P.; Giannakoudakis, D.A.; Amarasinghe, B.M.W.P.K.; Rajapaksha, A.U.; Kumara, P.T.P.; Triantafyllidis, K.S. and Vithanage, M. (2021). Propensity and appraisal of biochar performance in removal of oil spills: A comprehensive review. Environmental Pollution, 288, 117676.

Maki, R. and Qasim, B. (2023). Potassium hydroxide activated peanut shell as an effective adsorbent for the removal of zinc, lead and cadmium from wastewater. Journal of Ecological Engineering, 24(1), 66-78.

Obaid, S.A. (2020, November). Langmuir, Freundlich and Tamkin adsorption isotherms and kinetics for the removal aartichoke tournefortii straw from agricultural waste. In Journal of Physics: Conference Series (Vol. 1664, No. 1, p. 012011). IOP Publishing.

Ojedokun, A.T. and Bello, O.S. (2016). Sequestering heavy metals from wastewater using cow dung. Water Resources and Industry, 13, 7-13.

Paudel, S. and Shrestha, B. (2020). Adsorptive Removal of Iron (II) from Aqueous Solution Using Raw and Charred Bamboo Dust. International Journal of Advanced Social Sciences, 3(2), 27-35.

Prasath, R.R.; Muthirulan, P. and Kannan, N. (2014). Agricultural wastes as a low cost adsorbents for the removal of Acid Blue 92 dye: A comparative study with commercial activated carbon. IOSR Journal of Agriculture and Veterinary Science, 7(2), 19-32.

Sampranpiboon, P.; Charnkeitkong, P. and Feng, X. (2014). Equilibrium isotherm models for adsorption of zinc (II) ion from aqueous solution on pulp waste. WSEAS Transactions on Environment and Development, 10, 35-47.

Santuraki, A.H. and Muazu, A.A. (2015). Accessing the potential of Lonchocarpus laxiflorus roots (llr) plant biomass to remove Cadmium (II) ions from aqueous solutions: Equilibrium and kinetic studies. African Journal of Pure and Applied Chemistry, 9(5), 105-112.

Sharma, S. and Bhattacharya, A.J.A.W.S. (2017). Drinking water contamination and treatment techniques. Applied water science, 7(3), 1043-1067.

Vardhan, K.H.; Kumar, P.S. and Panda, R.C. (2019). A review on heavy metal pollution, toxicity and remedial measures: Current trends and future perspectives. Journal of Molecular Liquids, 290, 111197.

Vunain, E.; Mishra, A. K. and Mamba, B. B. (2016). Dendrimers, mesoporous silicas and chitosan-based nanosorbents for the removal of heavy-metal ions: A review. International journal of biological macromolecules, 86, 570-586.

Witek-Krowiak, A.; Szafran, R. G. and Modelski, S. (2011). Biosorption of heavy metals from aqueous solutions onto peanut shell as a low-cost biosorbent. Desalination, 265(1-3), 126-134.

Zheng, W.; Phoungthong, K.; Lü, F.; Shao, L.M. and He, P.J. (2013). Evaluation of a classification method for biodegradable solid wastes using anaerobic degradation parameters. Waste management, 33(12), 2632-2640.